Applied Microscopy
Korean Society of Microscopy
pISSN 2287-5123 · eISSN 2287-4445
http://dx.doi.org/10.9729/AM.2015.45.3.119

Review Article

Vapor Deposition Techniques for Synthesis of Two-Dimensional Transition Metal Dichalcogenides

Jeong-Gyu Song, Kyunam Park, Jusang Park, Hyungjun Kim*

School of Electrical and Electronic Engineering, Yonsei University, Seoul 03722, Korea

*Correspondence to:
Kim H,
Tel: +82-2-2123-5773
Fax: +82-2-313-2879
E-mail: hyungjun@yonsei.ac.kr

Received September 11, 2015
Revised September 13, 2015
Accepted September 13, 2015

Two-dimensional (2D) transition metal dichalcogenides (TMDCs) have attracted significant attention due to their unique and exotic properties attributed to their low dimensionality. In particular, semiconducting 2D TMDCs such as MoS_2, WS_2, $MoSe_2$, and WSe_2 have been demonstrated to be feasible for various advanced electronic and optical applications. In these regards, process to synthesize high quality 2D TMDCs layers with high reliability, wafer-scale uniformity, controllable layer number and excellent electronic properties is essential in order to use 2D TMDCs in practical applications. Vapor deposition techniques, such as physical vapor deposition, chemical vapor deposition and atomic layer deposition, could be promising processes to produce high quality 2D TMDCs due to high purity, thickness controllability and thickness uniformity. In this article, we briefly review recent research trend on vapor deposition techniques to synthesize 2D TMDCs.

Key Words: Molybdenum disulfide, Transition metal dichalcogenides, Two-dimensional materials, Chemical vapor deposition, Atomic layer deposition

INTRODUCTION

Transition metal dichalcogenides (TMDCs) are layered materials with strong in-plane covalent bonding and weak out-of-plane van der Waals bonding which is similar with graphene (Novoselov et al., 2005; Ramakrishna Matte et al., 2010). In particular, semiconducting two-dimensional (2D) TMDCs (MX_2: M=Mo, W and etc., X=S, Se, Te), exfoliated from bulk TMDCs, exhibit not only good chemical stability and flexibility but also unique electronic and optical properties, including indirect-to-direct band gap transition depending on layer number, high carrier mobility (approximately 100 cm^2/Vs) and strong spin-orbit coupling due to their broken inversion symmetry (Mak et al., 2010; Radisavljevic et al., 2011; Wang et al., 2012; Chhowalla et al., 2013; Song et al., 2013). These peculiar properties of 2D TMDCs make it promising to be used in field-effect transistors (Radisavljevic et al., 2011; Baugher et al., 2013; Georgiou et al., 2013; Lee et al., 2013), sensors (He et al., 2012; Li et al., 2012; Late et al., 2013; Liu et al., 2014a), photodetectors (Zhang et al., 2012; Lopez-Sanchez et al., 2013; Song et al., 2015), piezoelectric (Wu et al., 2014), and solar cell (Bernardi et al., 2013; Cheng et al., 2014; Furchi et al., 2014; Lee et al., 2014a) for future applications in such as wearable and flexible electronic devices which require compact, light-weight and high electrical and optical performance (Wang et al., 2012; Song et al., 2015).

One of the most important research field in 2D TMDCs is the reliable synthesis of 2D TMDCs with large area uniformity and layer number controllability. To date, the mechanical and chemical exfoliation methods have been employed to produce 2D TMDCs (Coleman et al., 2011; Eda et al., 2011;

This work was supported by the National Research Foundation of Korea (NRF) grant funded by the Korea government (MSIP) (No. NRF-2014R1A2A1A11052588), the Center for Integrated Smart Sensors funded by the Ministry of Science, ICT & Future Planning as Global Frontier Project (CISS-2011-0031848), Samsung Display Co., Ltd., and Korea Evaluation Institute of Industrial Technology (KEIT) funded by the Ministry of Trade, Industry and Energy (MOTIE) (Project No. 10050296, Large scale (Over 8") synthesis and evaluation technology of 2D chalcogenides for next generation electronic devices).

This is an open-access article distributed under the terms of the Creative Commons Attribution Non-Commercial License (http://creativecommons.org/licenses/by-nc/4.0) which permits unrestricted noncommercial use, distribution, and reproduction in any medium, provided the original work is properly cited.
Copyrights © 2015 by Korean Society of Microscopy

Radisavljevic et al., 2011; Li et al., 2012; Nicolosi et al., 2013). The exfoliated 2D TMDCs are suitable for basic research and demonstration of concept application since they have high crystallinity and inherent properties. However, the exfoliated 2D TMDCs have shown several limitations such as isolation, small size (usually less than a few μm), and low productivity, which make it difficult to be used 2D TMDCs in practical devices. Thus, significant efforts have been devoted to synthesize high quality and large area 2D TMDCs. Recently several studies have shown synthesis of 2D TMDCs using various methods based on the vapor deposition techniques: sulfurization of metal and metal oxide thin films (Lin et al., 2012; Zhan et al., 2012; Elías et al., 2013; Liu et al., 2014b), chemical vapor deposition (CVD) (Lee et al., 2012; Huang et al., 2013; Najmaei et al., 2013; van der Zande et al., 2013; Cong et al., 2014; Ji et al., 2014; Ling et al., 2014; Shaw et al., 2014; Dumcenco et al., 2015; Kang et al., 2015) and atomic layer deposition (ALD) (Song et al., 2013; Jin et al., 2014; Tan et al., 2014; Song et al., 2015). In this review, synthetic methods for 2D TMDCs, mainly focused on the MoS_2 and WS_2 which are the most studied 2D TMDCs, will be presented.

CHALCOGENIZATION OF METAL AND METAL OXIDE THIN FILM

Initial studies on the synthesis of 2D MoS_2 were focused on the sulfurization of Mo and MoO_x thin films, which were deposited by physical vapor deposition (PVD) at high temperature. Zhan et al. (2012) reported that the synthesis of MoS_2 film by thermal annealing (at 750°C) of PVD Mo thin film on SiO_2/Si substrate in sulfur vapor as shown in Fig. 1A-D. Similarly, Lin et al. (2012) reported wafer-scale (2 inch) MoS_2 thin layers synthesis by sulfurization of MoO_3 thin film at 1,000°C (Fig. 1E-G). Although these

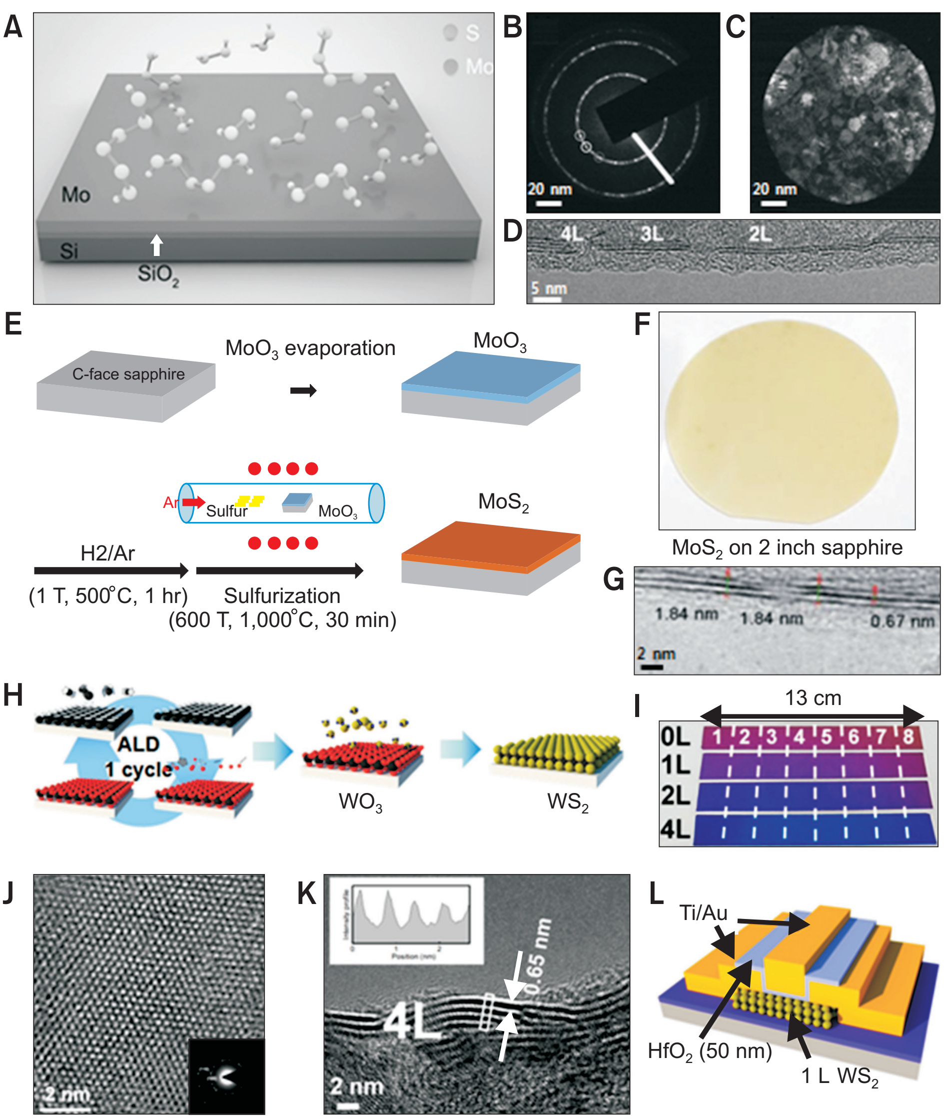

Fig. 1. (A) Schematic illustration of Mo sulfurization. (B) Diffraction pattern taken from MoS_2. (C) Dark field transmission electron microscopy (TEM) image of MoS_2. (D) Cross-sectional high-resolution TEM (HRTEM) image of MoS_2. (E) Synthesis procedure of MoO_3 sulfurization. (F) MoS_2 on a 2 inch sapphire wafer. (G) Cross-sectional HRTEM image of MoS_2. (H) Synthesis procedure for the atomic layer deposition (ALD) WO_3 sulfurization. (I) Large-area (approximately 13 cm) mono-, bi-, and tetralayer WS_2 on SiO_2 substrates. (J) A HRTEM image of a monolayer WS_2, and the diffraction pattern of WS_2 (inset). (K) Cross-sectional HRTEM image of tetralayer WS_2. (L) Field effect transistor structure based on WS_2. Fig. 1A-D reproduced from the article of Zhan et al. (2012) (*Small* 8, 966-971) with original copyright holder's permission. Fig. 1E-G reproduced from the article of Lin et al. (2012) (*Nanoscale* 4, 6637-6641) with original copyright holder's permission. Fig. 1H-L reproduced from the article of Song et al. (2013) (*ACS Nano* 7, 11333-11340) with original copyright holder's permission.

sulfurization methods are simple and easy to produce 2D MoS_2, several limitations exist such as difficulty in precise thickness control and in wafer-scale thickness uniformity of PVD Mo and MoO_x. Thus, precise control on the thickness of metal oxide film is essential to obtain layer number controlled, wafer-scale uniform 2D TMDCs. Recently, Song et al. (2013) demonstrated the synthesis of high quality WS_2 by the sulfurization of WO_3 thin film deposited by ALD. Since ALD has inherently excellent ability to control the film thickness over wafer scale, the synthesized WS_2 layer has retains the inherent benefits of the ALD process as well as high mobility of approximately 4 cm^2/Vs (Fig. 1H-L). Further, latest report by Song et al. (2015) has shown that the composition controllable synthesis of $Mo_{1-x}W_xS_2$ alloy using sulfurization of super-cycle ALD $Mo_{1-x}W_xO_y$. Based on this, they synthesized a vertically composition-controlled $Mo_{1-x}W_xS_2$ multilayer that has broadband light absorption. Since the various transition metal oxides can be easily deposited by ALD, sulfurization (or selenization) of ALD metal oxide could be extended to synthesis of various 2D TMDCs.

CHEMICAL VAPOR DEPOSITION

The synthesis of 2D TMDCs using CVD with metal oxide

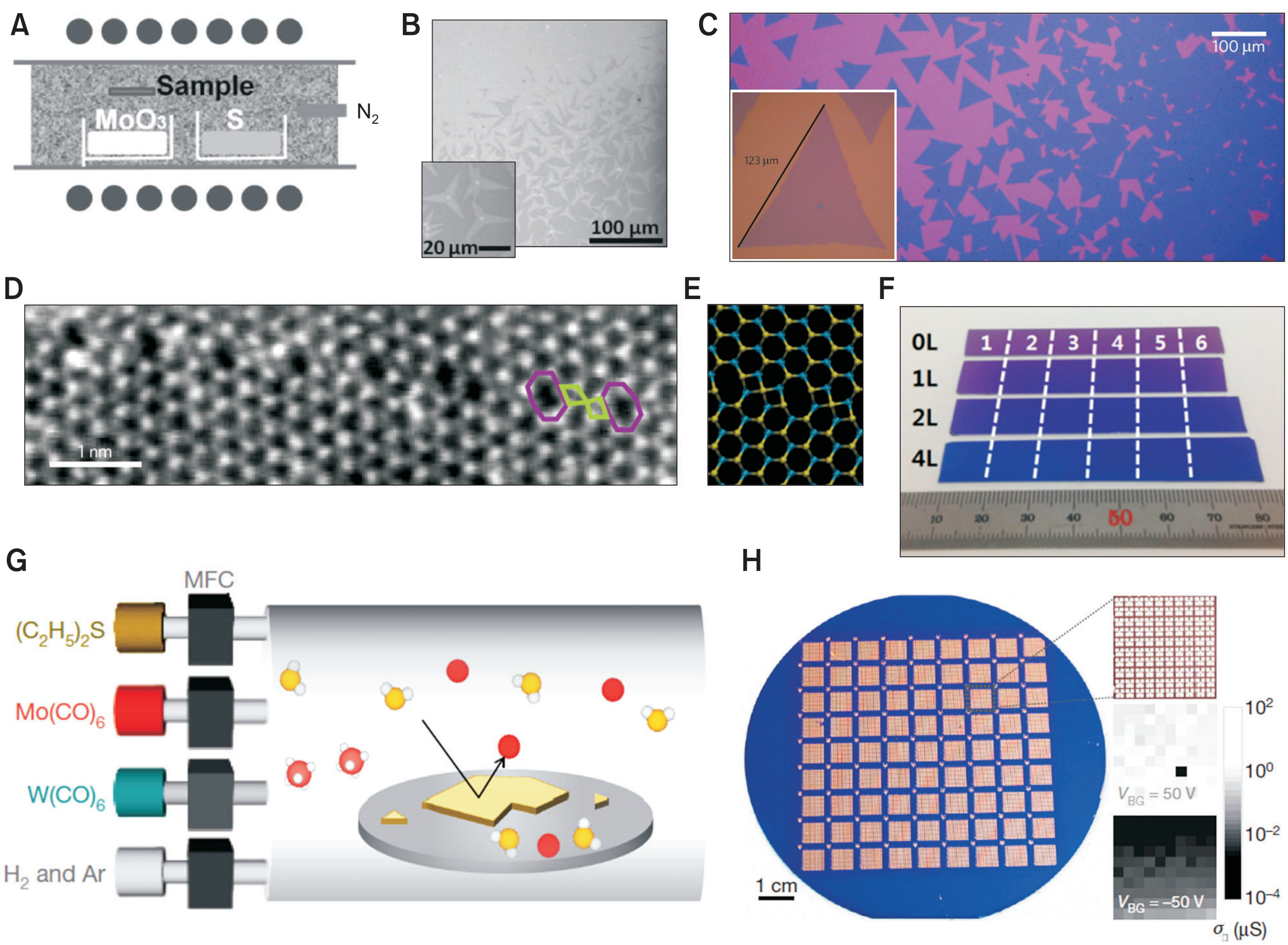

Fig. 2. (A) Schematic illustration of chemical vapor deposition (CVD) MoS_2. (B) The optical microscopy (OM) images of CVD MoS_2 on the SiO_2 substrate treated with reduce graphene oxide solution. (C) OM image of CVD MoS_2 on a SiO_2 substrate, and OM image of a monolayer CVD MoS_2 triangle with size up to 120 µm in lateral (inset). (D) High-resolution transmission electron microscopy image of the grain boundary of CVD MoS_2 with shown a periodic line of 8-4-4 ring defects. (E) An atomistic model of the experimental structure shown in Fig. 2D. (F) Large-area (1×7 cm^2) mono-, bi-, and tetralayered CVD WS_2 on SiO_2 substrates. (G) Schematic illustration of metal-organic CVD MoS_2 and WS_2. (H) Batch-fabricated 8×100 MoS_2 field effect transistor arrays on a 4-inch SiO_2 wafer. Top inset: enlarged image of one square containing 100 devices. Middle and bottom insets: corresponding color maps of $\sigma_□$ at gate bias V_{BG}=50 V and −50 V, respectively. Fig. 2A and B reproduced from the article of Lee et al. (2012) (*Advanced Materials* 24, 2320-2325) with original copyright holder's permission. Fig. 2C-E reproduced from the article of van der Zande et al. (2013) (*Nature Materials* 12, 554-561) with original copyright holder's permission. Fig. 2F reproduced from the article of Park et al. (2015) (*Nanoscale* 7, 1308-1313) with original copyright holder's permission. Fig. 2G and H reproduced from the article of Kang et al. (2015) (*Nature* 520, 656-660) with original copyright holder's permission.

(MO_3, M=Mo and W) and chalcogen (X=S and Se) powders at 600°C~700°C has been extensively studied (Lee et al., 2012; Najmaei et al., 2013; van der Zande et al., 2013; Ling et al., 2014). In this process scheme, MO_{3-x} is formed by the reduction of MO_3 vapor. Subsequently, MO_{3-x} vapor diffuses to the substrate and reacts with X vapor. Lee et al. (2012) reported the promotion of 2D MoS_2 synthesis using substrate treatment by graphene like species, such as reduced graphene oxide, perylene-3,4,9,10-tetracarboxylic acidtetrapotassium salt and perylene-3,4,9,10-tetracarboxylicdianhydride. Here, the species used for surface treatment promote act as seeds for 2D MoS_2 formation and enhance the lateral growth of MoS_2, as shown in Fig. 2A and B (Lee et al., 2012). Meanwhile, van der Zande et al. (2013) reported the synthesis of large MoS_2 single crystal grains (at 700°C) up to 120 μm without seeding. In this report, they used ultraclean substrates and fresh precursors to promote grain size (Fig. 2C). Further, they have observed that formation of periodic line of 8-4-4 ring defects at grain boundary of CVD MoS_2 as represented in Fig. 2D and E. Recent studies on the CVD with MO_3 and X powder have been focused on the synthesis of MoS_2 and WS_2 on single crystal substrate for enhancing grain size. In particular, orientation aligned growth of CVD MoS_2 on c-plane sapphire has been reported by Ji et al. (2014) and Dumcenco et al. (2015). They have shown that the same hexagonal lattice symmetry induces van der Waals epitaxy of MoS_2 on c-plane sapphire, which suggests possibility of wafer-scale growth of single-crystal MoS_2 similar with graphene on hydrogen-terminated germanium (Lee et al., 2014b).

However, the CVD process based on MO_3 and X powder is critically depending on process conditions such as amount of MO_3 and X powder, non-homogeneous diffusion of vaporized molecules, and outgoing flow of vapors from the chamber. Since these process conditions cannot be easily controlled, uniform and high quality synthesis is hardly achievable (Najmaei et al., 2013; van der Zande et al., 2013;

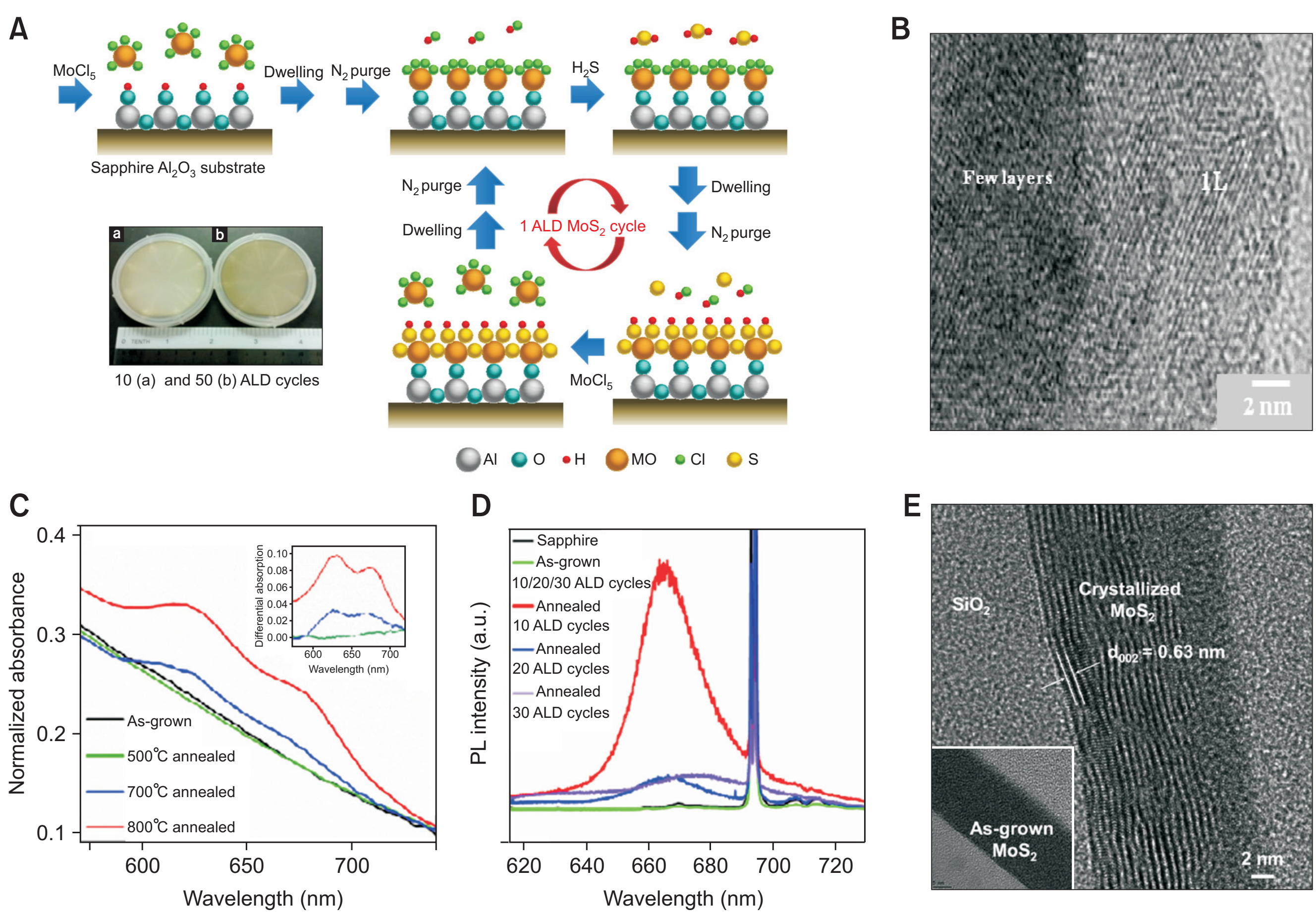

Fig. 3. (A) Schematic illustration of one growth cycle of atomic layer deposition (ALD) MoS_2. (B) High-resolution transmission electron microscopy (HRTEM) image of mono- and multilayer ALD MoS_2. (C) Optical absorption. (D) Photoluminescence spectra for ALD-deposited, as-grown or annealed MoS_2. (E) Cross-sectional HRTEM image of the ALD MoS_2 after annealed at 900°C for 5 minutes. Fig. 3A-D reproduced from the article of Tan et al. (2014) (*Nanoscale* 6, 10584-10588) with original copyright holder's permission. Fig. 3E reproduced from the article of Jin et al. (2014) (*Nanoscale* 6, 14453-14458) with original copyright holder's permission.

Park et al., 2015). Thus, CVD of 2D TMDCs based on gas precursor and reactant is more promising. As shown in Fig. 2F, Park et al. (2015) reported layer number controllable and wafer-scale uniform growth of WS_2 using WCl_6 and H_2S at 700°C. More recently, Kang et al. (2015) reported high quality WS_2 synthesis based on metal-organic CVD (MOCVD) using $Mo(CO)_6$, $W(CO)_6$, and $(C_2H_5)_2S$ at 550°C (Fig. 2G). The synthesized MOCVD 2D TMDCs exhibited homogeneous electrical properties with high electron mobility of 30 cm^2/Vs and 99% devices yield (Fig. 2H). However, the growth rate was reported to be very low, which requires 26 hours to grow monolayer 2D TMDCs.

ATOMIC LAYER DEPOSITION

Due to benefits of ALD in terms of thickness controllability of thin film in nanometer scale, ALD is considered to be a promising candidate to synthesis technique for 2D TMDCs. In fact, various ALD processes of chalcogenides thin films such as ZnS, GaS, CdS, etc, have been reported for photovoltaic and energy storage materials (Dasgupta et al., 2015). Recently, a few reports on ALD MoS_2 are available as shown in Fig. 3. Tan et al. (2014) reported growth of ALD MoS_2 film using $MoCl_5$ and H_2S at 300°C (Fig. 3A-D). In addition, low temperature (at 100°C) ALD MoS_2 process using $Mo(CO)_6$ and $(CH_3)_2S_2$ is

Table 1. Summary of the vapor deposition techniques for synthesis of two-dimensional TMDCs

TMDCs	Process	Process temperature (°C)	Layer number	Electrical properties ($cm^2V^{-1}s^{-1}$)	Reference
Chalcogenization of metal and metal oxide thin film					
MoS_2	Sulfurization (S powder) of PVD Mo (1~5 nm)	750	Mono- and few-layer mixing	Back gate FET Mobility: 0.004 to 0.04	Zhan et al. (2012)
	Sulfurization (S powder) of PVD MoO_3	1,000	Bi- and few-layer	Back gate FET Mobility: 0.8	Lin et al. (2012)
	Sulfurization (H_2S) of ALD MoO_3	Annealing: 1st, 600; 2nd, 1,000	Mono-, bi-, and tri-layer	-	Song et al. (2015)
WS_2	Sulfurization (S powder) of PVD WO_3	800	Mono-, bi-, and tri-layer	-	Elías et al. (2013)
	Sulfurization (H_2S) of ALD WO_3	1,000	Mono-, bi-, and tetra-layer	Top gate FET Mobility: 3.9	Song et al. (2013)
Chemical vapor deposition					
MoS_2	MoO_3 and S powder with seeding	650	Monolayer	Back gate FET Mobility: 0.02	Lee et al. (2012); Ling et al. (2014)
	MoO_3 and S powder	700	Monolayer	Back gate FET Mobility: 3 to 4	van der Zande et al. (2013)
	MoO_3 nanoribbons and S powder	850	Monolayer	Back gate FET Mobility: 4.3	Najmaei et al. (2013)
	MoO_3 and S powder	850	Monolayer on sapphire	Back gate FET Mobility: 0.1 to 1	Ji et al. (2014)
	MoO_3 and S powder	700	Monolayer on sapphire	Back gate FET Mobility: 25	Dumcenco et al. (2015)
WS_2	WO_3 and S powder	750	Monolayer	-	Cong et al. (2014)
	WCl_6 and H_2S gas	700	Mono-, bi-, and tetra-layer	-	Park et al. (2015)
MoS_2, WS_2	$Mo(CO)_6$, $W(CO)_6$, and diethyl sulfide	550	Monolayer	Top gate FET Mobility: 30	Kang et al. (2015)
$MoSe_2$	MoO_3 and Se powder	750	Mono- and few-layer	-	Shaw et al. (2014)
WSe_2	WO_3 and Se powder	750	Monolayer	Electric double-layer FET Mobility: 90	Huang et al. (2013)
Atomic layer deposition					
MoS_2	$Mo(CO)_6$ and dimethyl disulfide	100	Amorphous	-	Jin et al. (2014)
	$MoCl_5$ and H_2S gas	300	Amorphous	-	Tan et al. (2014)

TMDCs, transition metal dichalcogenides; PVD, physical vapor deposition; FET, field effect transistor; ALD, atomic layer deposition.

reported by Jin et al. (2014). However, the reported ALD MoS_2 films show low optical property attributed to amorphous phase as shown in Fig. 3E, which limits there use for the electrical and optical applications. The basic problem of ALD processes for TMDCs are the difficulty in the formation of layered structure. The deposition of high quality TMDCs by direct ALD process is yet to come.

CONCLUSIONS

This review provides a brief collection of literatures on the synthesis of 2D TMDCs materials as summarized in Table 1. Vapor deposition techniques, which are suitable for wafer-scale and high-quality synthesis of 2D TMDCs such as MoS_2, WS_2, WSe_2 and $MoSe_2$ for electronic and optoelectronic devices have been developed. To realize the advanced applications using 2D TMDCs, more efforts are needed to resolve many issues related to the growth, including high reliability, layer number controllability, wafer-scale uniformity and high crystallinity. Furthermore, synthesis of high quality 2D TMDCs will boost the study on the stacking of different types of 2D materials which could exhibit novel properties and new phenomena.

CONFLICT OF INTEREST

No potential conflict of interest relevant to this article was reported.

REFERENCES

Baugher B W H, Churchill H O H, Yang Y, and Jarillo-Herrero P (2013) Intrinsic electronic transport properties of high-quality monolayer and bilayer MoS2. *Nano Letters* **13**, 4212-4216.

Bernardi M, Palummo M, and Grossman J C (2013) Extraordinary sunlight absorption and 1 nm-thick photovoltaics using two-dimensional monolayer materials. *Nano Letters* **13**, 3664-3670.

Cheng R, Li D, Zhou H, Wang C, Yin A, Jiang S, Liu Y, Chen Y, Huang Y, and Duan X (2014) Electroluminescence and photocurrent generation from atomically sharp WSe2/MoS2 heterojunction pn diodes. *Nano Letters* **14**, 5590-5597.

Chhowalla M, Shin H S, Eda G, Li L J, Loh K P, and Zhang H (2013) The chemistry of two-dimensional layered transition metal dichalcogenide nanosheets. *Nature Chemistry* **5**, 263-275.

Coleman J N, Lotya M, O'Neill A, Bergin S D, King P J, Khan U, Young K, Gaucher A, De S, and Smith R J (2011) Two-dimensional nanosheets produced by liquid exfoliation of layered materials. *Science* **331**, 568-571.

Cong C, Shang J, Wu X, Cao B, Peimyoo N, Qiu C, Sun L, and Yu T (2014) Synthesis and optical properties of large-area single-crystalline 2D semiconductor WS2 monolayer from chemical vapor deposition. *Advanced Optical Materials* **2**, 131-136.

Dasgupta N P, Meng X, Elam J W, and Martinson A B (2015) Atomic layer deposition of metal sulfide materials. *Accounts of Chemical Research* **48**, 341-348.

Dumcenco D, Ovchinnikov D, Marinov K, Lazic P, Gibertini M, Marzari N, Sanchez O L, Kung Y C, Krasnozhon D, and Chen M W (2015) Large-area epitaxial monolayer MoS2. *ACS Nano* **9**, 4611-4620.

Eda G, Yamaguchi H, Voiry D, Fujita T, Chen M, and Chhowalla M (2011) Photoluminescence from chemically exfoliated MoS2. *Nano Letters* **11**, 5111-5116.

Elías A L, Perea-López N, Castro-Beltrán A, Berkdemir A, Lv R, Feng S, Long A D, Hayashi T, Kim Y A, Endo M, Gutiérrez H R, Pradhan N R, Balicas L, Mallouk T E, López-Urías F, Terrones H, and Terrones M (2013) Controlled synthesis and transfer of large-area WS2 sheets: from single layer to few layers. *ACS Nano* **7**, 5235-5242.

Furchi M M, Pospischil A, Libisch F, Burgdörfer J, and Mueller T (2014) Photovoltaic effect in an electrically tunable van der Waals heterojunction. *Nano Letters* **14**, 4785-4791.

Georgiou T, Jalil R, Belle B D, Britnell L, Gorbachev R V, Morozov S V, Kim Y J, Gholinia A, Haigh S J, and Makarovsky O (2013) Vertical field-effect transistor based on graphene-WS2 heterostructures for flexible and transparent electronics. *Nature Nanotechnology* **8**, 100-103.

He Q, Zeng Z, Yin Z, Li H, Wu S, Huang X, and Zhang H (2012) Fabrication of flexible MoS2 thin-film transistor arrays for practical gas-sensing applications. *Small* **8**, 2994-2999.

Huang J K, Pu J, Hsu C L, Chiu M H, Juang Z Y, Chang Y H, Chang W H, Iwasa Y, Takenobu T, and Li L J (2013) Large-area synthesis of highly crystalline WSe2 monolayers and device applications. *ACS Nano* **8**, 923-930.

Ji Q, Kan M, Zhang Y, Guo Y, Ma D, Shi J, Sun Q, Chen Q, Zhang Y, and Liu Z (2014) Unravelling orientation distribution and merging behavior of monolayer MoS2 domains on sapphire. *Nano Letters* **15**, 198-205.

Jin Z, Shin S, Kwon D H, Han S J, and Min Y S (2014) Novel chemical route for atomic layer deposition of MoS2 thin film on SiO2/Si substrate. *Nanoscale* **6**, 14453-14458.

Kang K, Xie S, Huang L, Han Y, Huang P Y, Mak K F, Kim C J, Muller D, and Park J (2015) High-mobility three-atom-thick semiconducting films with wafer-scale homogeneity. *Nature* **520**, 656-660.

Late D J, Huang Y K, Liu B, Acharya J, Shirodkar S N, Luo J, Yan A, Charles D, Waghmare U V, Dravid V P, and Rao C N R (2013) Sensing behavior of atomically thin-layered MoS2 transistors. *ACS Nano* **7**, 4879-4891.

Lee C H, Lee G H, van der Zande A M, Chen W, Li Y, Han M, Cui X, Arefe G, Nuckolls C, Heinz T F, Guo J, Hone J, and Kim P (2014a) Atomically thin p-n junctions with van der Waals heterointerfaces. *Nat Nano* **9**, 676-681.

Lee G H, Yu Y J, Cui X, Petrone N, Lee C H, Choi M S, Lee D Y, Lee C, Yoo W J, and Watanabe K (2013) Flexible and transparent MoS2 field-effect transistors on hexagonal boron nitride-graphene heterostructures. *ACS Nano* **7**, 7931-7936.

Lee J H, Lee E K, Joo W J, Jang Y, Kim B S, Lim J Y, Choi S H, Ahn S J, Ahn J R, and Park M H (2014b) Wafer-scale growth of single-crystal monolayer graphene on reusable hydrogen-terminated germanium. *Science* **344**, 286-289.

Lee Y H, Zhang X Q, Zhang W, Chang M T, Lin C T, Chang K D, Yu Y C, Wang J T W, Chang C S, Li L J, and Lin T W (2012) Synthesis of large-area MoS2 atomic layers with chemical vapor deposition. *Advanced Materials* **24**, 2320-2325.

Li H, Yin Z, He Q, Li H, Huang X, Lu G, Fam D W H, Tok A I Y, Zhang Q, and Zhang H (2012) Fabrication of single- and multilayer MoS2 film-based field-effect transistors for sensing NO at room temperature. *Small* **8**, 63-67.

Lin Y C, Zhang W, Huang J K, Liu K K, Lee Y H, Liang C T, Chu C W, and Li L J (2012) Wafer-scale MoS2 thin layers prepared by MoO3 sulfurization. *Nanoscale* **4**, 6637-6641.

Ling X, Lee Y H, Lin Y, Fang W, Yu L, Dresselhaus M S, and Kong J (2014) Role of the seeding promoter in MoS2 growth by chemical vapor deposition. *Nano Letters* **14**, 464-472.

Liu B, Chen L, Liu G, Abbas A N, Fathi M, and Zhou C (2014a) High-performance chemical sensing using schottky-contacted chemical vapor deposition grown monolayer MoS2 transistors. *ACS Nano* **5**, 5304-5314.

Liu H, Antwi K K A, Chua S, and Chi D (2014b) Vapor-phase growth and characterization of Mo1-xWxS2 ($0 \leq x \leq 1$) atomic layers on 2-inch sapphire substrates. *Nanoscale* **6**, 624-629.

Lopez-Sanchez O, Lembke D, Kayci M, Radenovic A, and Kis A (2013) Ultrasensitive photodetectors based on monolayer MoS2. *Nature Nanotechnology* **8**, 497-501.

Mak K F, Lee C, Hone J, Shan J, and Heinz T F (2010) Atomically thin MoS_ {2}: a new direct-gap semiconductor. *Physical Review Letters* **105**, 136805.

Najmaei S, Liu Z, Zhou W, Zou X, Shi G, Lei S, Yakobson B I, Idrobo J C, Ajayan P M, and Lou J (2013) Vapour phase growth and grain boundary structure of molybdenum disulphide atomic layers. *Nature Materials* **12**, 754-759.

Nicolosi V, Chhowalla M, Kanatzidis M G, Strano M S, and Coleman J N (2013) Liquid exfoliation of layered materials. *Science* **340**, 1226419.

Novoselov K, Jiang D, Schedin F, Booth T, Khotkevich V, Morozov S, and Geim A (2005) Two-dimensional atomic crystals. *Proceedings of the National Academy of Sciences of the United States of America* **102**, 10451-10453.

Park J, Lee W, Choi T, Hwang S H, Myoung J M, Jung J H, Kim S H, and Kim H (2015) Layer-modulated synthesis of uniform tungsten disulfide nanosheet using gas-phase precursors. *Nanoscale* **7**, 1308-1313.

Radisavljevic B, Radenovic A, Brivio J, Giacometti V, and Kis A (2011) Single-layer MoS2 transistors. *Nature Nanotechnology* **6**, 147-150.

Ramakrishna Matte H S S, Gomathi A, Manna A K, Late D J, Datta R, Pati S K, and Rao C N R (2010) MoS2 and WS2 analogues of graphene. *Angewandte Chemie* **122**, 4153-4156.

Shaw J C, Zhou H, Chen Y, Weiss N O, Liu Y, Huang Y, and Duan X (2014) Chemical vapor deposition growth of monolayer MoSe2 nanosheets. *Nano Research* **7**, 511-517.

Song J G, Park J, Lee W, Choi T, Jung H, Lee C W, Hwang S H, Myoung J M, Jung J H, and Kim S H (2013) Layer-controlled, wafer-scale, and conformal synthesis of tungsten disulfide nanosheets using atomic layer deposition. *ACS Nano* **7**, 11333-11340.

Song J G, Ryu G H, Lee S J, Sim S, Lee C W, Choi T, Jung H, Kim Y, Lee Z, Myoung J M, Dussarrat C, Lansalot-Matras C, Park J, Choi H, and Kim H (2015) Controllable synthesis of molybdenum tungsten disulfide alloy for vertically composition-controlled multilayer. *Nat Commun* **6**, 7817.

Tan L K, Liu B, Teng J H, Guo S, Low H Y, and Loh K P (2014) Atomic layer deposition of a MoS2 film. *Nanoscale* **6**, 10584-10588.

van der Zande A M, Huang P Y, Chenet D A, Berkelbach T C, You Y, Lee G H, Heinz T F, Reichman D R, Muller D A, and Hone J C (2013) Grains and grain boundaries in highly crystalline monolayer molybdenum disulphide. *Nature Materials* **12**, 554-561.

Wang Q H, Kalantar-Zadeh K, Kis A, Coleman J N, and Strano M S (2012) Electronics and optoelectronics of two-dimensional transition metal dichalcogenides. *Nature Nanotechnology* **7**, 699-712.

Wu W, Wang L, Li Y, Zhang F, Lin L, Niu S, Chenet D, Zhang X, Hao Y, and Heinz T F (2014) Piezoelectricity of single-atomic-layer MoS2 for energy conversion and piezotronics. *Nature* **514**, 470-474.

Zhan Y, Liu Z, Najmaei S, Ajayan P M, and Lou J (2012) Large-area vapor-phase growth and characterization of MoS2 atomic layers on a SiO2 substrate. *Small* **8**, 966-971.

Zhang C, Wang S, Yang L, Liu Y, Xu T, Ning Z, Zak A, Zhang Z, Tenne R, and Chen Q (2012) High-performance photodetectors for visible and near-infrared lights based on individual WS2 nanotubes. *Applied Physics Letters* **100**, 243101.